*ICIC Express Letters*
Volume **17**, Number **7**, July **2023**

ICIC International ©2023 ISSN 1881-803X
pp. 773–781

# INTEGRAL SFLOS PATH FOLLOWING CONTROL WITH HEADING BP NEURAL NETWORK BACKSTEPPING SLIDING-MODE CONTROLLER AND SPEED ADRC

Chengkai Wang and Ming Ji*

College of Intelligent Systems Science and Engineering
Harbin Engineering University
No. 145, Nantong Street, Nangang District, Harbin 150001, P. R. China
wck19971206@hrbeu.edu.cn; *Corresponding author: jimmouse2008@163.com

Received November 2022; accepted January 2023

Abstract. *A path following control strategy is proposed, which consists of speed active disturbance rejection nonlinear feedback controller, heading BPNN backstepping sliding-mode controller and integral Serret-Frenet line-of-sight (SFLOS) guidance law. When a ship is sailing, it often deviates from the predetermined track due to the disturbance of sea wind, waves and currents. In this paper, firstly, an accurate 4-DOF ship dynamic model is established, including the external disturbances. Then, active disturbance rejection speed controller which adopts non-linear extended state observer (NLESO) to estimate sum disturbance, and heading backstepping sliding-mode controller in which back propagation neural network (BPNN) is used to fit the nonlinear function in the model are designed. On this basis, anti-windup integral SFLOS guidance law is designed to compensate the negative influence of ocean current and sideslip on ship track tracking. Finally, the results of simulation and ship model experiment show that the ship path following control strategy proposed in this paper has excellent stability and performance.*
**Keywords:** Ship path following, Integral SFLOS, Extended state observer, BP neural network, Sliding-mode control

1. **Introduction.** In recent years, with the continuous exploration of the ocean, the problem of ship path following control has gradually become one of the important directions in the field of ship control. Ship track control is of great significance for transportation, communication, construction, rescue and other tasks. The disturbance of wind, wave and ocean current is one of the main reasons for ships to deviate from the scheduled route [1]. In addition, underactuated and nonlinear characteristic and parameters uncertainties also bring great difficulties to the study of ship maneuverability [2].

At present, the indirect path tracking control method is widely used [3], which uses guidance law to calculate the desired heading (and sometimes the speed) according to the tracking error, and then use a controller to control the heading and speed. Line-of-sight (LOS) guidance law has been widely used in this field, which is proposed by Fossen in [4]. Integral LOS (ILOS) proposed in [5,6] can compensate tracking error caused by constant ocean current. Then, in [7], adaptive integral LOS (AILOS) was presented, which can estimate ocean current vector and compensate it, and backstepping heading controller based on RBFNN was designed. Improved adaptive integral LOS (IAILOS) can estimate not only ocean current vector but sideslip angle and eliminate tracking error caused by them, which was proposed in [2,8]. In addition, fuzzy logic system is used to compensate dynamic uncertainties and external disturbances, and backstepping attitude and speed controller combined with tracking differentiators are designed.

DOI: 10.24507/icicel.17.07.773

In Section 2, a 4-DOF ship dynamic model has been proposed for control strategy design and simulation. In Section 3, speed active disturbance rejection nonlinear feedback controller and BPNN heading sliding-mode controller is designed. According to the drawbacks of ILOS, AILOS and IAILOS, anti-windup integral LOS guidance law which can prevent integral saturation is proposed. Moreover, in Section 4, the simulation and ship model experiment result shows the practicability of the ship path following control system. Finally, in Section 5, we conclude the paper.

2. **Ship Motion Mathematical Model.** NED coordinate system and body coordinate system are often used in the study of ship maneuverability to represent the position and attitude of the ship, which are represented as $\{n\} = (x_n, y_n, z_n)$ and $\{b\} = (x_b, y_b, z_b)$ in Figure 1, respectively [8,9].

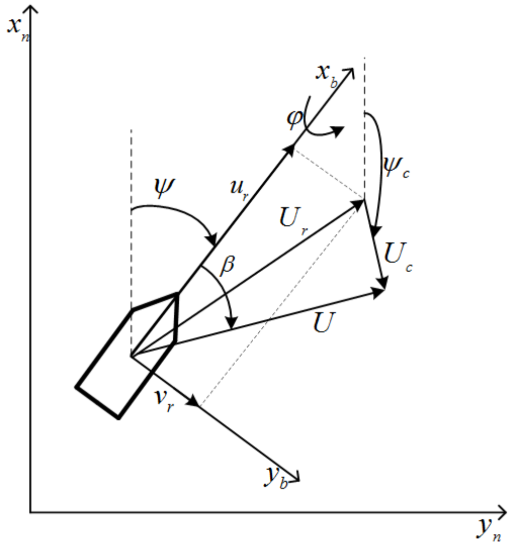


Figure 1. Reference system and some variables

Usually, the study of ship maneuverability needs to take surge, sway and yaw into account, while ignoring the effects of roll, pitch and heave. In this paper, the effect of roll is also taken into account to evaluate safety and comfort. The influence of ocean currents is also considered. Therefore, 4-DOF kinematics equation is as follows:

$$\begin{cases} \dot{x} = u_r \cos\psi - v_r \cos\varphi \sin\psi + U_c \cos\psi_c \\ \dot{y} = u_r \sin\psi + v_r \cos\varphi \cos\psi + U_c \sin\psi_c \\ \dot{\varphi} = p \\ \dot{\psi} = r\cos\varphi \end{cases} \tag{1}$$

where $u_r = u - U_c \cos(\psi_c - \psi)$, $v_r = v - U_c \sin(\psi_c - \psi)$.

Pérez and Blanke presented a 4-DOF ship dynamics mathematical model including surge, sway, yaw and roll in [10] with hydrodynamic derivatives, which was based on the experiment results of roll planar motion mechanism facility of Danish Maritime Institute.

$$\begin{cases} m(\dot{u}_r - v_r r - x_G r^2 + z_G pr) = X_{hyd} + X_{prop} + X_{cs} + X_{ext} \\ m(\dot{v}_r - z_G \dot{p} + x_G \dot{r} + u_r r) = Y_{hyd} + Y_{prop} + Y_{cs} + Y_{ext} \\ I_{xx}\dot{p} - m z_G(\dot{v}_r + u_r r) = K_{hyd} + K_{prop} + K_{cs} + K_{ext} \\ I_{zz}\dot{r} + m x_G(\dot{v}_r + u_r r) = N_{hyd} + N_{prop} + N_{cs} + N_{ext} \end{cases} \tag{2}$$

where $m$ is the mass of the ship, $I_{xx}$ and $I_{zz}$ are the moment of inertia of the ship around the $x_b$ axis and the $z_b$ axis respectively, $x_G$ and $z_G$ are coordinates of ship's center of gravity in body coordinate system, the subscripts *hyd*, *prop*, *cs*, *ext* represent hydrodynamic force, propeller force, rudder force and external disturbance force, respectively. For more about hydrodynamic force and rudder force, see [10]. This paper assumes that the propeller has only thrust along the $x_b$ axis, that is,

$$\begin{cases} X_{prop} = (1 - t_P)\, \rho n^2 D_P^4 K_T\,(J_P)\, n^2 \\ Y_{prop} = 0,\ K_{prop} = 0,\ N_{prop} = 0 \end{cases} \tag{3}$$

where $t_P$ is thrust deduction coefficient, $\rho$ is density of seawater, $n$ is speed of propeller, $D_P$ is diameter of propeller, $J_P$ is velocity coefficient, $K_T(J_P)$ is thrust coefficient.

Tristan Pérez and Mogens blanke also gave a simplified mathematical model of the steering mechanism in [10], which is described by a first-order differential equation.

$$T_\delta \dot{\delta} + \delta = \delta_c \tag{4}$$

with bounded rudder angle $|\delta| \leq \delta^*$ and bounded rudder angular velocity $\left|\dot{\delta}\right| \leq \mu^*$, where $\delta^* > 0$, $\mu^* > 0$, $T_\delta$ is time constant of steering engine, and $\delta_c$ is command rudder angle.

3. **Design of Path-Following Control Strategy.** In this paper, an indirect track tracking method is proposed, and the structure of the control system is shown in Figure 2. The reference heading $\psi_d$ is calculated by using the integral SFLOS guidance law and speed $U_{rd} \in R^+$. Then, the heading BPNN backstepping sliding-mode controller and speed active disturbance rejection nonlinear feedback controller are designed, respectively.

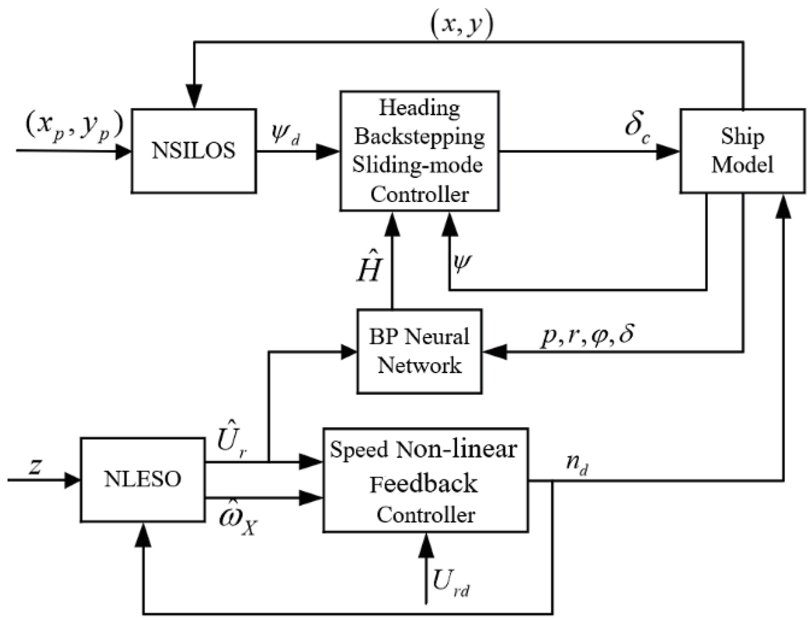


Figure 2. Structure block diagram of control system

3.1. **Speed active disturbance rejection nonlinear feedback controller.** According to first equation of Equation (2), and only fluid inertia force, navigation resistance and propeller thrust are considered, while other components of force along the $x_b$ axis are regarded as disturbances $\omega_1$, that is,

$$(m - X_{\dot{u}})\, \dot{u}_r = X_{uu} u_r^2 + (1 - t_P)\, \rho D_P^4 K_T\,(J_P)\, n^2 + \omega_1 \tag{5}$$

where $X_{\dot{u}}$ is added mass along $x_b$ axis, and $X_{uu}$ is damping coefficient.

However, $K_T(J_P)$ is difficult to calculate, and when Equation (3) is simplified to a linear function of $n^2$ as shown below

$$X'_{prop} = (1 - t_P)\, \rho D_P^4 k_{prop} n^2 \tag{6}$$

and choose an appropriate value for the positive constant $k_{prop}$, the thrust error $\omega_2 = X_{prop} - X'_{prop}$ is small. The thrust relative error surface at different speeds and propeller speeds is shown in Figure 3.

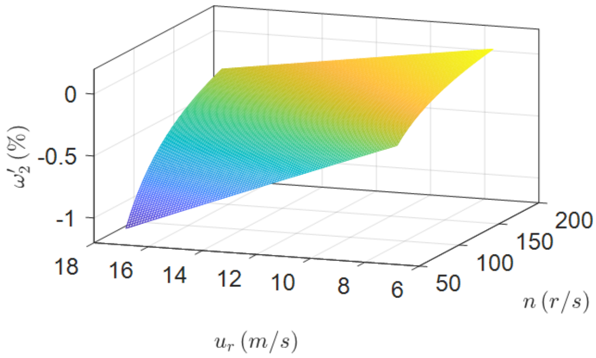


FIGURE 3. (color online) Thrust relative error surface

Considering the disturbance $\omega_3$ caused by the speed error $\tilde{n} = n_d - n$ of propeller and the disturbance $\omega_4$ caused by the error between relative velocity $U_r$ and relative surge velocity $u_r$, Equation (5) is further simplified to

$$(m - X_{\dot{u}})\,\dot{U}_r = X_{uu}U_r^2 + (1 - t_P)\,\rho D_P^4 k_{prop} n_d^2 + \omega_X \tag{7}$$

where $\omega_X = \sum_{i=1}^{4} \omega_i$ is sum disturbance force.

In this section, NLESO which is the core of active disturbance rejection technology, is first designed to estimate $U_r$ and $\omega_X$, and then, a nonlinear feedback control law is designed on this basis.

Define the expanded state vector $\boldsymbol{x} = [x_1, x_2]^T = [U_r, \omega_X]^T$, system input $u_x = n_d^2$ and $z$ is the measured value of $U_r$. According to Equation (7), the NLESO can be expressed as follows:

$$\begin{cases} \dot{\hat{x}}_1 = \dfrac{\hat{x}_2}{m - X_{\dot{u}}} + \dfrac{X_{uu}}{m - X_{\dot{u}}}\hat{x}_1^2 + \alpha_1\,(z - \hat{x}_1) + \dfrac{(1 - t_P)\rho D_P^4 k_{prop}}{m - X_{\dot{u}}} u_x \\ \dot{\hat{x}}_2 = \alpha_2\,\mathrm{fal}\,(z - \hat{x}_1, \eta, \gamma) \end{cases} \tag{8}$$

where $\alpha_1$, $\alpha_2$, $\eta$, $\gamma$ are positive constant parameters, and nonlinear function $\mathrm{fal}(x, \eta, \gamma)$ is defined as

$$\mathrm{fal}(x, \eta, \gamma) = \begin{cases} |x|^\eta \cdot \mathrm{sign}(x), & |x| > \gamma \\ x/\gamma^\eta, & |x| \le \gamma \end{cases} \tag{9}$$

Define relative velocity error $e_U = U_{rd} - U_r$ and $\hat{e}_U = U_{rd} - \hat{x}_1$ and design the nonlinear feedback control law as $\dot{\hat{e}}_U = -k_{11}\mathrm{atan}\,(k_{12}e_U)$, so that

$$n_d = \sqrt{\frac{(m - X_{\dot{u}})\,\dot{U}_{rd} - X_{uu}\hat{x}_1^2 - \hat{x}_2 + k_{11}\mathrm{atan}\,(k_{12}e_U)}{(1 - t_P)\,\rho D_P^4 k_{prop}}} \tag{10}$$

where constant parameters $k_{11}, k_{12} \in R^+$.

3.2. **Heading BPNN backstepping sliding-mode controller.** Rewrite the fourth equation of Equation (2) and equation for calculating rudder moment in [10] as

$$\ddot{\psi} + H(U_r, p, r, \varphi, \delta) = K\delta \tag{11}$$

where $H\,(U_r, p, r, \varphi, \delta)$ is a nonlinear function describing steering characteristics, and $K$ is a constant parameter. As the expression of $H\,(U_r, p, r, \varphi, \delta)$ is hard to obtain accurately, it is a good idea to use BPNN, which is shown in Figure 4, to estimate it as $\hat{H}\,(U_r, p, r, \varphi, \delta)$.

BP neural network is usually trained by random gradient descent method, see [11] for more. And the historical navigation data of ships can be used for off-line training of neural

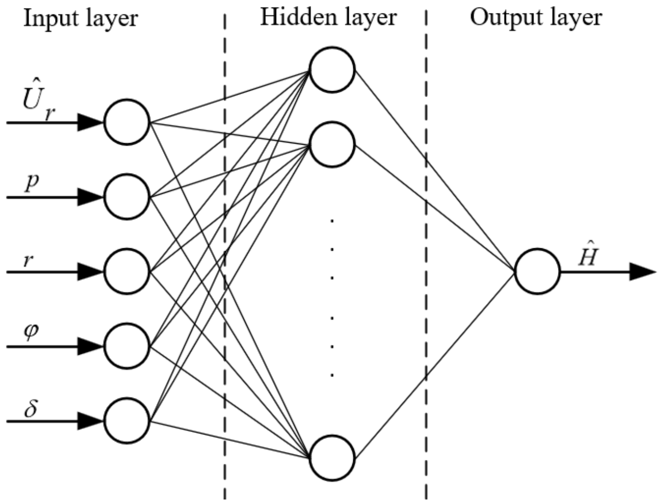


FIGURE 4. Structure of BP neural network

networks. When the BP neural network can well estimate $H(U_r, p, r, \varphi, \delta)$, it can be used for heading control.

Define the heading tracking error $\psi_e = \psi_d - \psi$ and sliding surface as

$$s = \psi_e + c\dot{\psi}_e = 0 \tag{12}$$

where constant $c \in R^+$ is a design parameter, which means the rate at which $\psi_e$ converges to zero. Consider the Lyapunov function $V_1 = s^2/2$ and its derivative is $\dot{V}_1 = s\dot{s} = \dot{\psi}_d + c\ddot{\psi}_d - r + cH(U_r, p, r, \varphi, \delta)$. Design the virtual control law as $\dot{s} = -k_{21}s - k_{22}\text{sign}(s)$, where $k_{21}, k_{22} \in R^+$ are design parameters, so that $\dot{V}_1 = -k_{21}s^2 - k_{22}s^2/|s| < 0$ and the virtual control variable can be obtained as

$$\delta' = \left[\dot{\psi}_d + c\ddot{\psi}_d - r + c\hat{H}(U_r, p, r, \varphi, \delta) + k_{21}s + k_{22}\text{sign}(s)\right] \Big/ (cK) \tag{13}$$

Define the rudder angle error as $\delta_e = \delta' - \delta$. According Equation (4) and Lyapunov function $V_2 = V_1 + \delta_e^2/2$, design the control law as follows

$$\delta_c = Tk_3\delta' + T\dot{\delta}' + (1 - Tk_{23})\,\delta \tag{14}$$

where $k_{23} \in R^+$ is a design parameter, so that it can be obtained that $\dot{V}_2 = \dot{V}_1 - k_{23}\delta_e^2 < 0$.

3.3. **Integral SFLOS guidance law.** In this section, an integral SFLOS guidance law that can compensate for current disturbance and sideslip is proposed which can guide the ship to follow a curve path desired, which is as shown in Figure 5. The desired path $(x_p, y_p)$ is determined by the parameter $\theta$, and path direction angle $\psi_p = \text{atan2}(\partial y_p/\partial\theta, \partial x_p/\partial\theta)$. The following error is defined as

$$\begin{cases} x_e = (x - x_p)\cos\psi_p + (y - y_p)\sin\psi_p \\ y_e = -(x - x_p)\sin\psi_p + (y - y_p)\cos\psi_p \end{cases} \tag{15}$$

Design the update law of $\theta$ and desired heading

$$\dot{\theta} = [V_r\cos(\psi - \psi_p) + k_\theta x_e] \Big/ \sqrt{x_{p'}^2 + y_{p'}^2} \tag{16}$$

$$\psi_d = \psi_p + \psi_{int} - \text{atan}(y_e/\Delta) \tag{17}$$

where $k_\theta \in R^+$ is a design parameter.

The disturbance of ship position caused by sideslip and ocean current is mainly in the low frequency band, so the following integration term $\psi_{int}$ can be used to compensate for the disturbance on track tracking

$$\psi_{int} = \int g(y_e)\text{d}t \tag{18}$$

where $|\psi_{int}| \le \psi_{int}^*$ and

$$g(y_e) = \begin{cases} y_e, & |y_e| \le y_e^* \\ 0, & \text{else} \end{cases} \tag{19}$$

are used to prevent integral saturation.

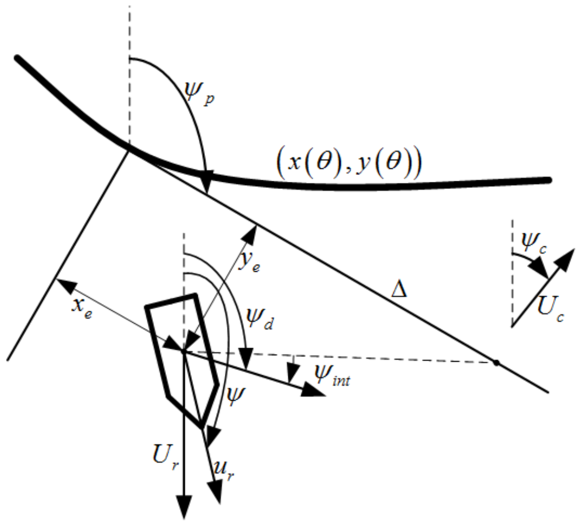


FIGURE 5. Integral SFLOS guidance law

4. **Simulation and Experiment Result.** A container ship is selected as the simulation object, $L_{pp} = 230.66$ m and $\nabla = 46070$ m$^3$. The initial conditions for simulation are $(x_0, y_0) = (0, 300)$, $U_{r0} = 8$ m/s and $\psi_0 = 45°$. The direction and speed of ocean current are $U_c = 1 + 0.5\sin(2\pi t/3600 + \pi/3)$ m/s and $\psi_c = 75°$. The significant wave height $h_{1/3} = 2.2$ m and the wind speed $U_w = 12$ m/s. And the desired speed $U_{rd} = 12$ m/s.

In this paper, two control strategies are used for simulation. Strategy 1 is the control strategy proposed in this paper. And strategy 2 uses PID heading controller, PID speed controller and SFLOS guidance law. The simulation results are shown in Figures 6-10.

As illustrated in the simulation of Figure 6 and Figure 7, both control strategies can make the ship converge to the desired path. However, control strategy 1 converges more rapidly, and eliminates sideslip and ocean current disturbance more effectively than control strategy 2, so the tracking error is smaller. According to Figure 8, speed active disturbance

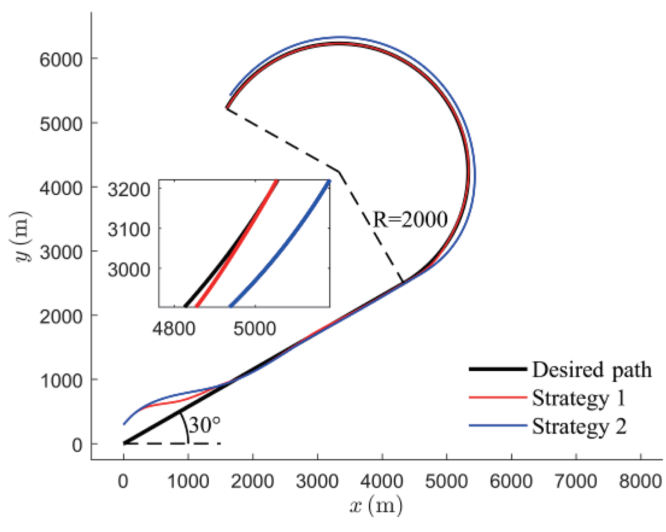


FIGURE 6. Ship track

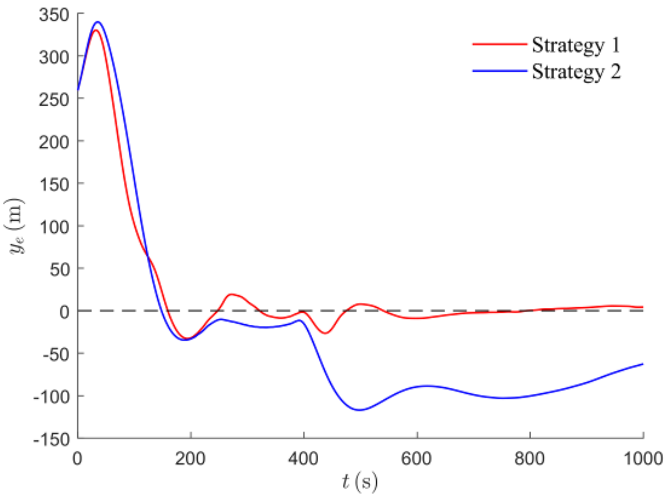


FIGURE 7. Tracking error

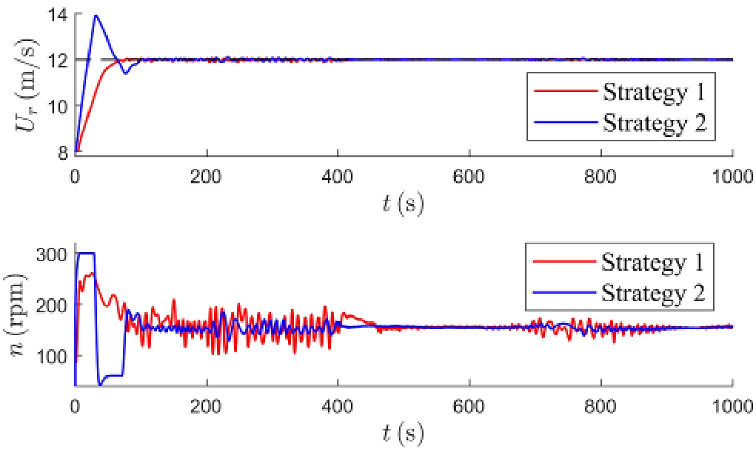


FIGURE 8. Relative velocity and propeller speed

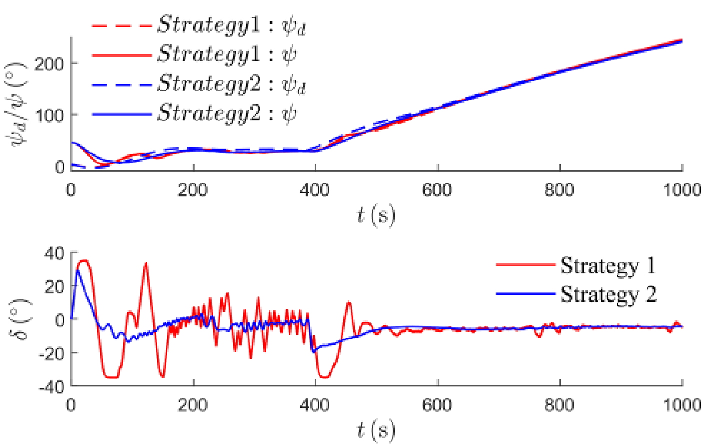


FIGURE 9. Heading and rudder angle

rejection nonlinear feedback controller has shorter setting time than PID controller, and the transition process is smooth without overshoot, but the fluctuation of propeller speed is larger than that of PID controller because the propeller eliminates the disturbance observed by NLESO. And as shown in Figure 9, Heading BPNN backstepping sliding-mode controller can make the ship track the desired heading better than PID controller.

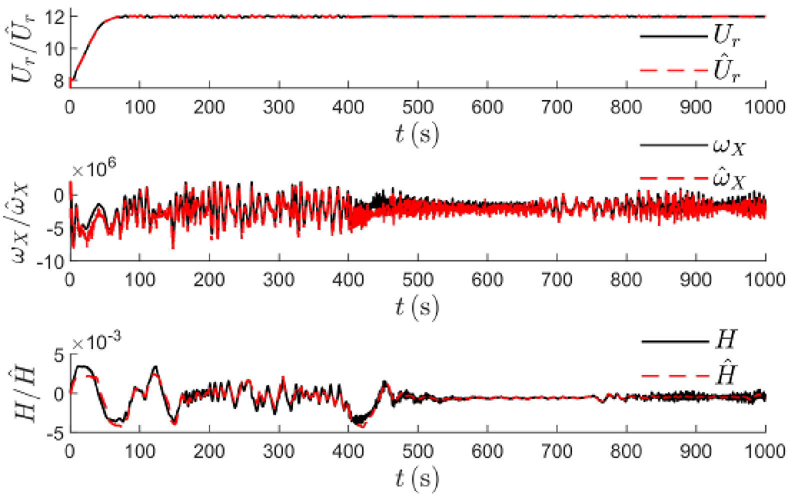


FIGURE 10. Estimates of ESO and BPNN

FIGURE 11. Ship model used for test

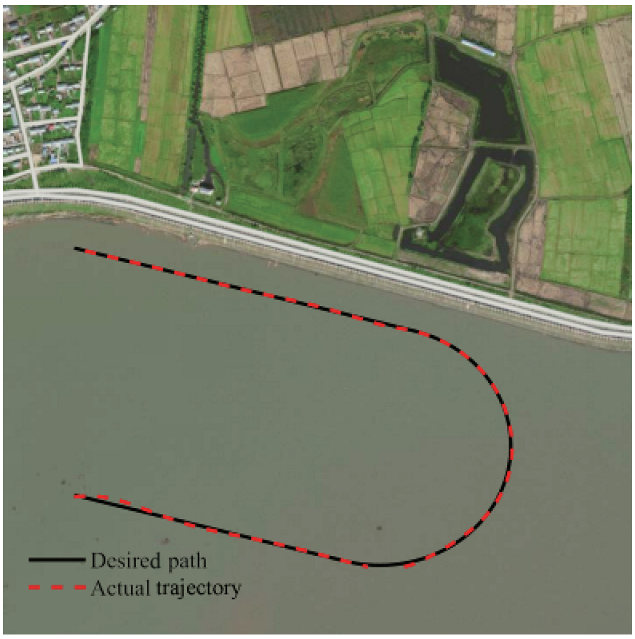


FIGURE 12. Ship model path following test

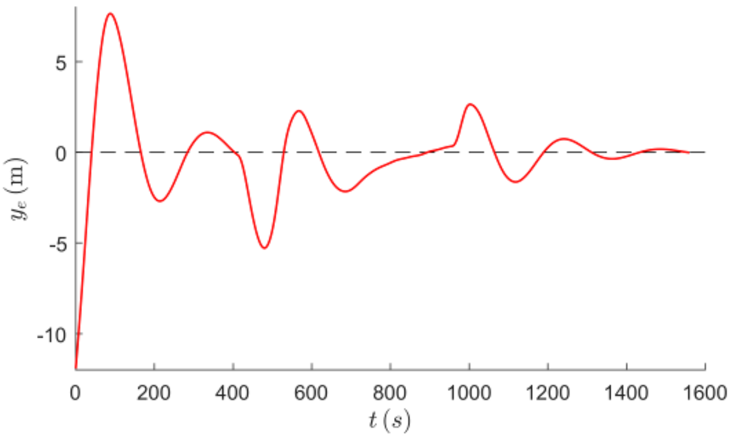


FIGURE 13. Ship model test tracking error

In order to better verify the performance of the control strategy proposed in this paper, a ship model with GPS and compass, as shown in Figure 11, is used to do a navigation test in the Songhua River whose $L_{pp} = 6.5$ m and $\nabla = 0.9$ m$^3$. The desired speed $U_{rd}$ is set to 0.4 m/s. In Figure 12 and Figure 13, obviously, the actual trajectory of the ship roughly coincides with the desired path, and the tracking error is kept within 8 m.

5. **Conclusions.** In this paper, a strategy that can effectively realize ship track control is proposed. The simulation result shows the availability and good control performance of the presented strategy. Ship model navigation test also shows the practicability of the control strategy.

Because most of the factors that cause the ship to deviate from the path are slow time-varying, and the integral term is very effective for low-frequency interference, so it has broad prospects for development. However, the dynamic process is easy to deteriorate due to integral terms, so some improvements are still needed.

## REFERENCES

[1] Y. Huang, Y. Hu, J. Wu and W. Huang, Practical observer-based path following control of the guide ship with propeller and rudder in the underway replenishment, *Ships and Offshore Structures*, vol.17, no.3, pp.506-517, 2022.
[2] Y. Su, L. Wan, D. Zhang and F. Huang, An improved adaptive integral line-of-sight guidance law for unmanned surface vehicles with uncertainties, *Applied Ocean Research*, vol.108, 102488, 2021.
[3] X. Han and X. Zhang, Trajectory tracking control based on closed-loop gain shaping algorithm, *Journal of Harbin Engineering University*, vol.41, no.11, pp.1629-1635, 2020.
[4] T. I. Fossen, Line-of-sight path-following control utilizing an extended Kalman filter for estimation of speed and course over ground from GNSS positions, *Journal of Marine Science and Technology (Japan)*, vol.27, no.1, pp.806-813, 2022.
[5] M. Lin, Z. Zhang, Y. Pang, H. Lin and Q. Ji, Underactuated USV path following mechanism based on the cascade method, *Scientific Reports*, vol.12, no.1, 2022.
[6] B. Min and X. Zhang, Concise robust fuzzy nonlinear feedback track keeping control for ships using multi-technique improved LOS guidance, *Ocean Engineering*, vol.224, 108734, 2021.
[7] Z. Zheng and Y. Zou, Adaptive integral LOS path following for an unmanned airship with uncertainties based on robust RBFNN backstepping, *ISA Transactions*, vol.65, pp.210-219, 2016.
[8] J. Nie and X. Lin, Improved adaptive integral line-of-sight guidance law and adaptive fuzzy path following control for underactuated MSV, *ISA Transactions*, vol.94, pp.151-163, 2019.
[9] T. I. Fossen, *Handbook of Marine Craft Hydrodynamics and Motion Control*, John Wiley Sons, Ltd., 2011.
[10] T. Pérez and M. Blanke, *Mathematical Ship Modeling for Control Application*, https://www.researchgate.net/publication/266576717, 2015.
[11] S. Zhao, W. Li and W. Zhang, Active disturbance rejection control for ship trajectory based on radial basis function neural network, *Journal of Shanghai Maritime University*, vol.41, no.4, pp.20-24, 2020.